

Electronic Supplementary Information for

**A Unique Series of Chromium(III) Mono-alkynyl Complexes Supported by Tetraazamacrocycles**

Ashley J. Schuman <sup>a</sup>, Sarah F. T. Robey <sup>a</sup>, Eileen C. Judkins <sup>a</sup>, Matthias Zeller <sup>a</sup> and Tong Ren<sup>\*a</sup>

---

\* To whom correspondence should be addressed. E-mail: [tren@purdue.edu](mailto:tren@purdue.edu)

<sup>a</sup> Department of Chemistry, Purdue University, West Lafayette, Indiana 47907

## Table of Contents

1. Synthetic details	
<b>Table S1.</b> Total percent yield of <b>1a – 4a</b> .....	S3
2. X-ray structural analysis	
<b>Table S2.</b> Crystallographic data for <b>1a – 4a, 3b, and 4b</b> .....	S7
<b>Figure S1.</b> ORTEP plot of <b>2a</b> with Np disorder .....	S7
<b>Figure S2.</b> ORTEP plot of <b>3b</b> .....	S8
<b>Figure S3.</b> ORTEP plot of <b>4b</b> .....	S8
<b>Table S3.</b> Selected bond lengths and angles for <b>3b and 4b</b> .....	S9
3. Absorption details	
<b>Figure S4.</b> UV-vis absorption spectra of <b>1b – 4b</b> .....	S10
<b>Figure S5.</b> UV-vis absorption spectra of <b>1a – 4a</b> .....	S10
<b>Table S4.</b> Vibronic progression analysis of <b>1a – 4a, 3b, and 4b</b> .....	S11
4. IR characterization	
<b>Figure S6.</b> FTIR of complexes <b>1b – 4b</b> .....	S12
<b>Figure S7.</b> FTIR of complexes <b>1a – 4a</b> .....	S12
5. Emission studies	
<b>Figure S8.</b> Time-delayed phosphorescence spectrum for <b>1a</b> .....	S13
<b>Figure S9.</b> Time-delayed phosphorescence spectrum for <b>2a</b> .....	S13
<b>Figure S10.</b> Time-delayed phosphorescence spectrum for <b>3a</b> .....	S14
<b>Figure S11.</b> Time-delayed phosphorescence spectrum for <b>4a</b> .....	S14
<b>Figure S12.</b> Time-delayed phosphorescence spectrum for <b>3b</b> .....	S15
<b>Figure S13.</b> Time-delayed phosphorescence spectrum for <b>4b</b> .....	S15
<b>Figure S14.</b> Emission spectra of <b>1a</b> at RT and 77 K .....	S16
<b>Figure S15.</b> Emission spectra of <b>2a</b> at RT and 77 K .....	S16
<b>Figure S16.</b> Emission spectra of <b>3a</b> at RT and 77 K .....	S17
<b>Figure S17.</b> Emission spectra of <b>4a</b> at RT and 77 K .....	S17
<b>Figure S18.</b> Emission spectra of <b>3b</b> at RT and 77 K .....	S18
<b>Figure S19.</b> Emission spectra of <b>4b</b> at RT and 77 K .....	S18
6. References	

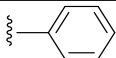
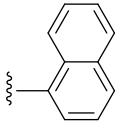
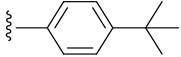
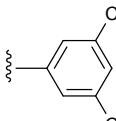
## Synthetic details

***Trans-[Cr(meso-HMC)(C<sub>2</sub>Ph)Cl]Cl via lithiation ([1a]Cl).*** The reaction between 0.336 g of *trans*-[Cr(*meso*-HMC)Cl<sub>2</sub>]Cl (0.76 mmol) and 1.2 equivalents of LiC<sub>2</sub>Ph yielded 0.0407 g of [1a]Cl (0.08 mmol, 11% based on Cr) after recrystallization from CH<sub>2</sub>Cl<sub>2</sub>/CH<sub>3</sub>OH and Et<sub>2</sub>O.

***Cis-[Cr(rac-HMC)(C<sub>2</sub>Ph)Cl]Cl via lithiation.*** The reaction between 0.500 g of *cis*-[Cr(*rac*-HMC)Cl<sub>2</sub>]Cl (1.13 mmol) and 0.95 equivalents of LiC<sub>2</sub>Ph yielded 0.0013 g of *cis*-[Cr(*rac*-HMC)(C<sub>2</sub>Ph)Cl]Cl after recrystallization from CH<sub>2</sub>Cl<sub>2</sub>/Et<sub>2</sub>O (0.003 mmol, 0.23% based on Cr) and 0.1682 g of *cis*-[Cr(*rac*-HMC)Cl<sub>2</sub>]Cl were recovered.

***Cis-[Cr(rac-HMC)(C<sub>2</sub>Ph)Cl]Cl via acid degradation.*** 0.100 g of *cis*-[Cr(*rac*-HMC)(C<sub>2</sub>Ph)<sub>2</sub>]Cl (0.174 mmol) were dissolved in CH<sub>3</sub>OH and 1.0 mL of a 0.12 M HCl methanol solution (0.127 mmol, 0.7 equivalents) were added. The solution immediately became more purple in color. The reaction was left to stir for approximately 30 minutes, upon which there appeared to be no solid formation. ESI-MS showed complete conversion to the desired product. The solvent was removed via rotary evaporation and the residue was dissolved in CH<sub>2</sub>Cl<sub>2</sub>. A purple-gray solid was precipitated with the addition of Et<sub>2</sub>O, yielding 0.0787 g (0.15 mmol, 89% based on Cr). Recrystallization was attempted from CH<sub>3</sub>OH/Et<sub>2</sub>O and CH<sub>2</sub>Cl<sub>2</sub>/Et<sub>2</sub>O, however, a teal blue solid gradually appeared, indicating the formation of *cis*-[Cr(HMC)Cl<sub>2</sub>]Cl.

**Table S1.** Total percent yield of 1a – 4a based on Cr in *trans*-[Cr(HMC)Cl<sub>2</sub>]OTf

Complex	Aryl	Total Yield
1a		48%
2a		67%
3a		51%
4a		35%

## X-Ray structural analysis

Single crystals of **[1a]Cl** and **3a** were grown *via* slow diffusion of Et<sub>2</sub>O into a concentrated CH<sub>3</sub>OH solution. Single crystals of **2a**, **4a**, and **4b** were grown *via* vapor diffusion (**2a**) or slow diffusion (**4a** and **4b**) of Et<sub>2</sub>O into a concentrated solution of CH<sub>3</sub>CN. Single crystals of **3b** were grown *via* slow diffusion of hexanes into a concentrated solution of CH<sub>2</sub>Cl<sub>2</sub>. X-ray diffraction data for **[1a]Cl** were collected on a Nonius KappaCCD diffractometer using Mo K $\alpha$  ( $\lambda = 0.71073$  Å) at 200 K. Data were collected using the Nonius Collect software<sup>1</sup>, processed using HKL3000<sup>2</sup> and data were corrected for absorption and scaled using Scalepack.<sup>2</sup> The structure of **[1a]Cl** was solved using the structure solution program PATTY in DIRDIF99<sup>3</sup>. Data for **2a**, **4a**, and **4b** were collected at 150 K on a Bruker Quest diffractometer with a fixed chi angle, a sealed tube fine focus X-ray tube with Mo K $\alpha$  radiation ( $\lambda = 0.71073$  Å), single crystal curved graphite incident beam monochromator, a Photon II area detector, and an Oxford Cryosystems low temperature device. Data for **3a** and **3b** were collected at 150 K on a Bruker Quest diffractometer with kappa geometry, an I- $\mu$ -S microsource X-ray tube, laterally graded multilayer (Goebel) mirror for monochromatization, a Photon-II (**3b**) or Photon-III (**3a**) area detector and an Oxford Cryosystems low temperature device. with Cu K $\alpha$  radiation ( $\lambda = 1.54178$  Å). Data for **2a**, **3a**, **4a**, **3b**, and **4b** were collected and processed using APEX3<sup>4</sup> and reduced using SAINT, space groups were assigned using XPREP within the SHELXTL<sup>5</sup> suite of programs, solved using ShelXS<sup>6</sup> (**2a**, **3a**, **3b**, **4a**) or ShelXM<sup>6</sup> (**4b**). All structures were refined using Shelxl2018 and the graphical interface Shelxle.<sup>7-9</sup> If not specified otherwise, H atoms attached to carbon and nitrogen atoms, as well as hydroxyl hydrogens, were positioned geometrically and constrained to ride on their parent atoms. C-H bond distances were constrained to 0.95 Å for aromatic, and to 1.00, 0.99 and 0.98 Å for aliphatic C-H, CH<sub>2</sub> and CH<sub>3</sub> moieties, respectively. O-H distances of alcohols were constrained to 0.84 Å. Methyl CH<sub>3</sub> hydroxyl H atoms were allowed to rotate but not to tip to best fit the experimental electron density.  $U_{\text{iso}}(\text{H})$  values were set to a multiple of  $U_{\text{eq}}(\text{C})$  with 1.5 for CH<sub>3</sub> and OH, and 1.2 for C-H, CH<sub>2</sub> and N-H units, respectively.

If not specified otherwise, H atoms attached to carbon and nitrogen atoms, as well as hydroxyl hydrogens, were positioned geometrically and constrained to ride on their parent atoms. C-H bond distances were constrained to 0.95 Å for aromatic, and to 1.00, 0.99 and 0.98 Å for aliphatic C-H, CH<sub>2</sub> and CH<sub>3</sub> moieties, respectively. O-H distances of alcohols were constrained to 0.84 Å. Ammonium N-H distances were either constrained to 1.00 Å (**1a**, **3a**, **3b**, **4a**), or the H atom positions were freely refined (**2a**, **4b**). Methyl CH<sub>3</sub> hydroxyl H atoms were allowed to rotate but not to tip to best fit the experimental electron density.  $U_{\text{iso}}(\text{H})$  values were set to a multiple of  $U_{\text{eq}}(\text{C/N/O})$  with 1.5 for CH<sub>3</sub> and OH, and 1.2 for C-H, CH<sub>2</sub> and N-H units, respectively, with the exception of  $U_{\text{iso}}(\text{H})$  values for ammonium H atoms of **4b**, which were freely refined.

### Special refinement details of **[1a]Cl**

In complex **[1a]Cl**, an OMIT command was used to remove reflections with high error. The methanol solvate molecule is disordered and refined to occupy two positions.  $U^{ij}$  components of their ADPs were restrained to be similar (SIMU command). The C-O bond distances were

restrained to a target value of 1.43 Å (DFIX). The positions of the H1A and H1B atoms of the O-H group were restrained to a target value of 2.1 and 2.5 Å from the Cl2 counteranion, respectively. Subject to these conditions the occupancy rates refined to be 0.49(1) and 0.51(1).

### Special refinement details of 2a

In complex **2a**, the ethynyl naphthalene ligand is disordered and is refined to occupy two positions. The two disordered moieties were restrained to have similar bond angles and lengths (SAME command).  $U^{ij}$  components of their ADPs were restrained to be similar (SIMU command). Subject to these conditions, the occupancy rates refined to be 0.576(3) and 0.424(3). A hydrogen bond exists between O3 of the triflate counteranion and N1 of the macrocyclic ligand. An OMIT command was used to remove a reflection with high error.

### Special refinement details of 3a

In complex **3a**, the Cr, HMC macrocycle, and Cl are disordered and is refined to occupy three positions. The three disordered moieties were restrained to have similar bond angles and lengths (SAME command).  $U^{ij}$  components of their ADPs were restrained to be similar (SIMU command). A SUMP command was used to constrain the occupancies of the three components to unity. Subject to these conditions the occupancy rates refined to be 0.406(1), 0.361(3), and 0.233(3).

The tert-butyl group on the tert-butylphenylacetylene ligand is disordered and is refined to occupy two positions. The two disordered moieties were restrained to have similar bond angles and lengths (SAME command).  $U^{ij}$  components of their ADPs were restrained to be similar (SIMU command). Subject to these conditions the occupancy rates refined to be 0.548(9) and 0.452(9).

The triflate counteranion is disordered and is refined to occupy three positions with the SO<sub>3</sub> unit always pointing towards the N-H groups of the macrocycle and the methanol solvate molecules. The three disordered moieties were restrained to have the same S-O, C-F, and C-O bond distances (SADI command).  $U^{ij}$  components of their ADPs were restrained to be similar (SIMU command). A hydrogen bond exists between O1B of the triflate counteranion and N1C of the macrocyclic ligand. Subject to these conditions the occupancy rates refined to be 0.541(3), 0.250(3), and 0.209(3).

The methanol solvent molecule is disordered and is refined to occupy three positions. The C-O bond distances were restrained to a target value (DFIX). The O-H groups are restrained to be H-bonded to the SO<sub>3</sub> groups of the triflate counteranion. The methyl H atoms were first refined with HFIX 137 (rotating) and then with AFIX 3 (pure riding). Subject to these conditions the occupancy rates refined to be 0.406(1), 0.406(1), and 0.188(3).

### Special refinement details of 4a

In complex **4a**, the dichlorophenyl phenyl moiety of the dichlorophenylacetylene substituent is disordered extensively. Disorder over four orientations, differing mostly by rotation around the acetylene axis, was refined. A SUMP command was used to constrain the occupancies of the four components of the ligand to unity. The four disordered moieties were restrained to have similar bond angles and lengths (SAME command). A SADI command was used to restrain the C2-C3 bond lengths to be similar within the four disordered ligand parts. The phenyl rings were restrained to be planar (FLAT command).  $U^{ij}$  components of their ADPs were restrained to be similar (SIMU command). Subject to these conditions the occupancy rates refined to be 0.310(3), 0.333(3), 0.0634(16), and 0.294(3).

A diethyl ether solvent molecule, adjacent to the disordered dichlorophenyl phenyl moiety, was refined as disordered over two mutually exclusive positions. A DFIX command was used to restrain equivalent C-O and C-C bond lengths within the molecule to target values. A SAME command was used to restrain the bond angles and lengths of the two disordered component to be similar to each other.  $U^{ij}$  components of ADPs were restrained to be similar for all disordered atoms. Subject to these conditions the occupancy ratios refined to 0.652(5) and 0.348(5).

The triflate counteranion was refined as disordered over two orientations by a "wiggle" movement of the SO<sub>3</sub> unit. A SAME command was used to restrain the bond angles and lengths of the two disordered component to be similar to each other.  $U^{ij}$  components of their ADPs were restrained to be similar (SIMU command). Subject to these conditions the occupancy ratios refined to 0.618(9) and 0.382(9).

### Special refinement details of 3b

In complex **3b**, one tert-butyl alkynyl substituent in the structure is ca. 1:1 disordered. The substituent is disordered by a rotation of the tert-butyl group and an upwards bend of the phenylene ring.

The two parts of the disordered ligand were restrained to have similar bond angles and lengths as observed in the non-disordered ligand (SAME command).  $U^{ij}$  components of their ADPs were restrained to be similar (SIMU command). The atoms C3 and C3B were constrained to have identical positions (EXYZ) and same anisotropic displacement parameters (EADP). Subject to these conditions the occupancy ratio refined to 0.546(7) to 0.454(7).

### Special refinement details of 4b

In complex **4b**, an OMIT command was used to omit reflections with high error.

**Table S2.** Crystal data for mono-alkynyl complexes **1a**, **2a**, **3a**, and **4a** and bis-alkynyl complexes **3b** and **4b**

	[1a]Cl	2a	3a	4a	3b	4b
chemical formula	C <sub>25</sub> H <sub>45</sub> Cl <sub>2</sub> CrN <sub>4</sub> O	C <sub>31</sub> H <sub>46</sub> ClCrF <sub>3</sub> N <sub>5</sub> O <sub>3</sub> S	C <sub>30</sub> H <sub>53</sub> ClCrF <sub>3</sub> N <sub>4</sub> O <sub>4</sub> S	C <sub>89</sub> H <sub>150</sub> Cl <sub>9</sub> Cr <sub>3</sub> F <sub>9</sub> N <sub>13</sub> O <sub>12</sub> S <sub>3</sub>	C <sub>41</sub> H <sub>62</sub> CrF <sub>3</sub> N <sub>4</sub> O <sub>3</sub> S	C <sub>35</sub> H <sub>45</sub> Cl <sub>4</sub> CrF <sub>3</sub> N <sub>5</sub> O <sub>3</sub> S
fw, g/mol	540.55	713.24	710.27	2336.44	800.00	866.62
space group	<i>C</i> 2/ <i>c</i> (No. 15)	<i>P</i> 2 <sub>1</sub> / <i>c</i> (No. 14)	<i>P</i> $\bar{1}$ (No. 2)	<i>P</i> $\bar{3}$ (No. 147)	<i>P</i> 2 <sub>1</sub> / <i>n</i> (No. 14)	<i>P</i> $\bar{1}$ (No. 2)
<i>a</i> , Å	29.5012(5)	16.7207(8)	11.3221(5)	24.2698(6)	15.3929(15)	9.838(2)
<i>b</i> , Å	11.5356(2)	12.2764(6)	13.1665(6)	24.2698(6)	13.5965(12)	13.224(4)
<i>c</i> , Å	16.5203(4)	17.8968(8)	14.2387(7)	11.2278(4)	22.0346(16)	17.386(4)
$\alpha$ °	90	90	64.220(2)	90	90	93.298(16)
$\beta$ °	91.120(1)	110.330	69.482(3)	90	109.307	105.918(16)
$\gamma$ °	90	90	72.759(3)	120	90	107.430(16)
<i>V</i> , Å <sup>3</sup>	5621.02(19)	3444.8(3)	1763.81(15)	5727.4(3)	4352.3(7)	2051.0(9)
<i>Z</i>	8	4	2	2	4	2
<i>T</i> , K	200	150	150	150	150	150
$\lambda$ , Å	0.71073	0.71073	1.54178	0.71073	1.54178	0.71073
$\rho_{\text{calcd}}$ , g/cm <sup>3</sup>	1.278	1.375	1.337	1.355	1.221	1.403
<i>R</i>	0.075	0.040	0.069	0.055	0.075	0.042
<i>R</i> <sub>w</sub> ( <i>F</i> <sup>2</sup> )	0.246	0.113	0.220	0.155	0.233	0.125

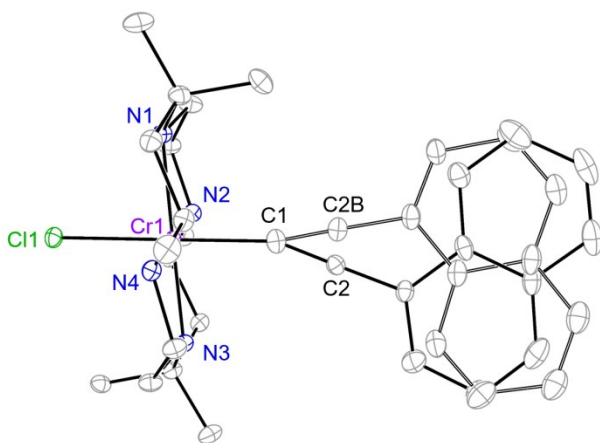


**Figure S1.** ORTEP plot of **2a** at 30% probability level with both disordered C<sub>2</sub>Np fragments. H atoms and the <sup>-</sup>OTf counteranion were omitted for clarity.

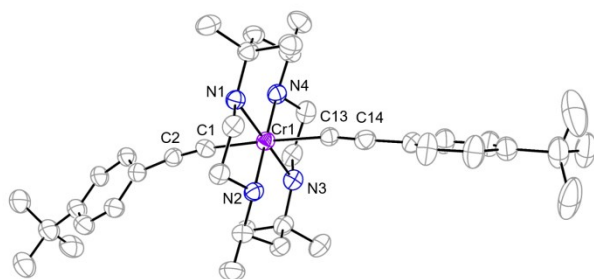


**Figure S2.** ORTEP plot of **3b** at 30% probability level. H atoms and the  $^-OTf$  counteranion were omitted for clarity.

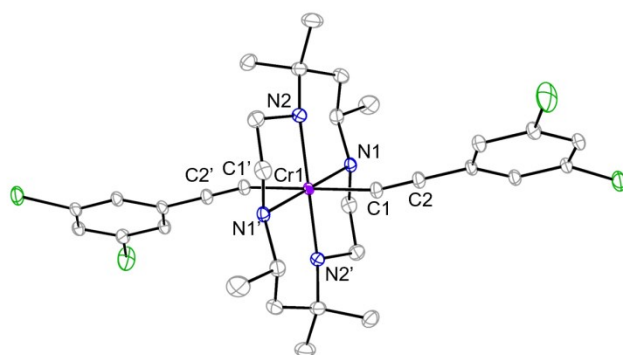


**Figure S3.** ORTEP plot of **4b** at 30% probability level. H atoms and the  $^-OTf$  counteranion were omitted for clarity.



**Table S3.** Selected bond lengths (Å) and bond angles (°) for **3b** and **4b**

	<b>3b</b>	<b>4b<sup>a</sup></b>
<b>Cr1-N1</b>	2.065(3)	2.0815(12)
<b>Cr1-N2</b>	2.097(4)	2.0910(13)
<b>Cr1-N3</b>	2.074(3)	-
<b>Cr1-N4</b>	2.093(3)	-
<b>Cr1-C1</b>	2.085(7)	2.0745(13)
<b>Cr1-C13</b>	2.123(5)	-
<b>C1-C2</b>	1.17(1)	1.2223(16)
<b>C13-C14</b>	1.137(8)	-
<b>C1-Cr1-C1</b>	-	180.00(6)
<b>C1-Cr1-C13</b>	177.1(2)	-
<b>Cr1-C1-C2</b>	172.4(5)	166.12(2)
<b>Cr1-C13-C14</b>	170.6(4)	-
<b>N1-Cr1-N3</b>	179.4(1)	-
<b>N2-Cr1-N4</b>	179.5(2)	-
<b>N1-Cr1-N2</b>	84.8(2)	84.68(5)
<b>N1-Cr1-N2'</b>	-	95.32(5)
<b>N1-Cr1-N4</b>	95.3(1)	-
<b>N2-Cr1-N3</b>	94.6(2)	-
<b>N3-Cr1-N4</b>	85.3(1)	-

<sup>a</sup>The unit cell revealed two crystallographically independent molecules; geometric parameters for only one of them are listed here.

## Absorption details

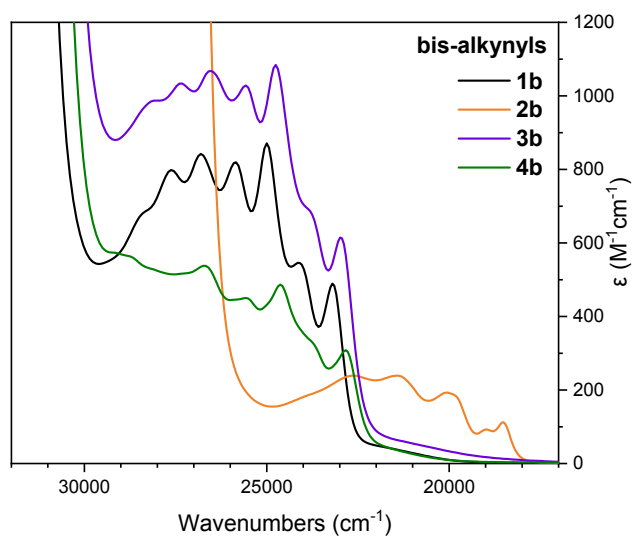


**Figure S4.** UV-vis absorption spectra of *trans*-[Cr(HMC)(C<sub>2</sub>Ar)<sub>2</sub>]OTf complexes as CH<sub>2</sub>Cl<sub>2</sub> solutions, where Ar = Ph (black), Np (orange), C<sub>6</sub>H<sub>4</sub>tBu (purple), and 3,5-Cl<sub>2</sub>C<sub>6</sub>H<sub>3</sub> (green).

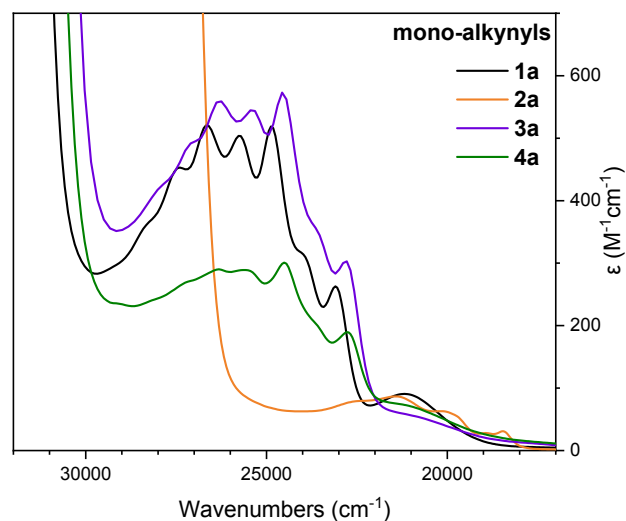


**Figure S5.** UV-vis absorption spectra of *trans*-[Cr(HMC)(C<sub>2</sub>Ar)Cl]OTf complexes as CH<sub>2</sub>Cl<sub>2</sub> solutions, where Ar = Ph (black), Np (orange), C<sub>6</sub>H<sub>4</sub>tBu (purple), and 3,5-Cl<sub>2</sub>C<sub>6</sub>H<sub>3</sub> (green).

**Table S4.** Vibronic progression analysis of **1a – 4a, 3b, and 4b**

	<b>Peaks Considered, cm<sup>-1</sup></b>	<b>Vibronic Progression, cm<sup>-1</sup></b>
<b>1a</b>	27397.26 26666.67 25773.19 24875.62 23980.81 23094.69	730.59 893.48 897.57 894.81 886.12
<b>2a</b>	22624.43 21413.27 20080.32 18939.39 18450.18	1211.16 1332.95 1140.93 489.21
<b>3a</b>	27173.91 26385.22 25445.29 24570.02 23640.66 22831.05	788.69 939.93 875.27 929.36 809.61
<b>4a</b>	26315.79 25575.45 24509.80 23696.68 22779.04	740.34 1065.65 813.12 917.64
<b>3b</b>	27322.40 26525.20 25575.45 24752.48 23923.44 22988.51	797.20 949.75 822.97 829.04 934.93
<b>4b</b>	26737.97 25575.45 24630.54 23866.35 22831.05	1162.52 944.91 764.19 1035.3

## IR characterization

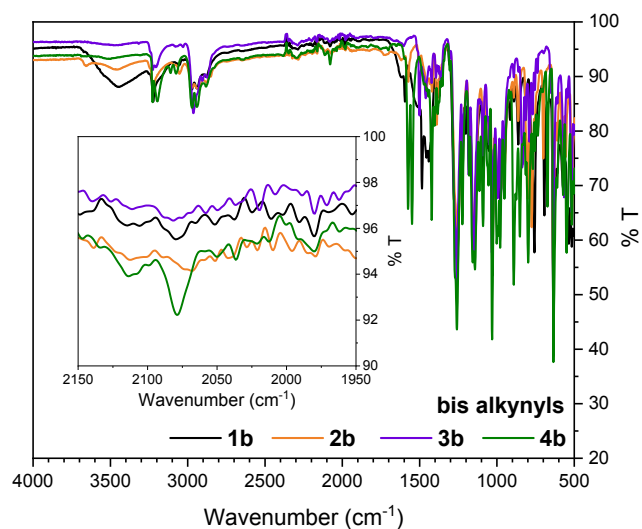


**Figure S6.** FTIR of *trans*-[Cr(HMC)(C<sub>2</sub>Ar)<sub>2</sub>]OTf complexes, where Ar = Ph (black), Np (orange), C<sub>6</sub>H<sub>4</sub>tBu (purple), and 3,5-Cl<sub>2</sub>C<sub>6</sub>H<sub>3</sub> (green).

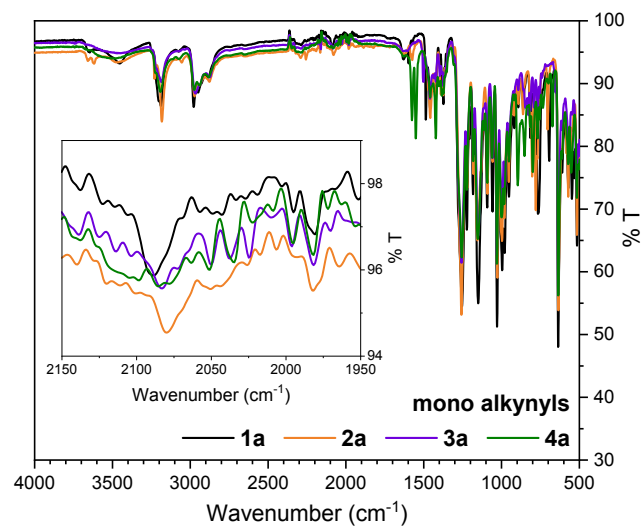


**Figure S7.** FTIR of *trans*-[Cr(HMC)(C<sub>2</sub>Ar)Cl]OTf complexes, where Ar = Ph (black), Np (orange), C<sub>6</sub>H<sub>4</sub>tBu (purple), and 3,5-Cl<sub>2</sub>C<sub>6</sub>H<sub>3</sub> (green).

## Emission studies

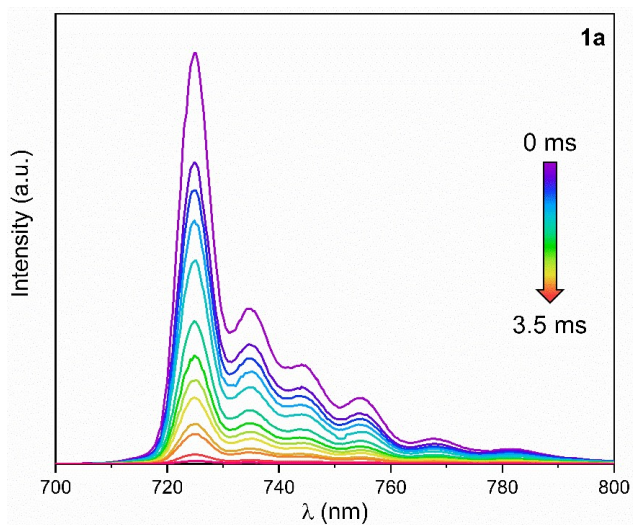


**Figure S8.** Time-delayed phosphorescence spectrum for **1a** in 4:1  $\text{CH}_3\text{CH}_2\text{OH}:\text{CH}_3\text{OH}$  glass at 77 K and varying delay times.

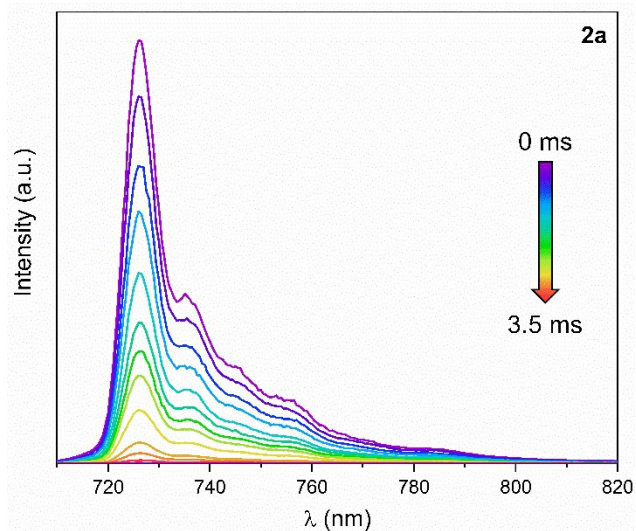


**Figure S9.** Time-delayed phosphorescence spectrum for **2a** in 4:1  $\text{CH}_3\text{CH}_2\text{OH}:\text{CH}_3\text{OH}$  glass at 77 K and varying delay times.

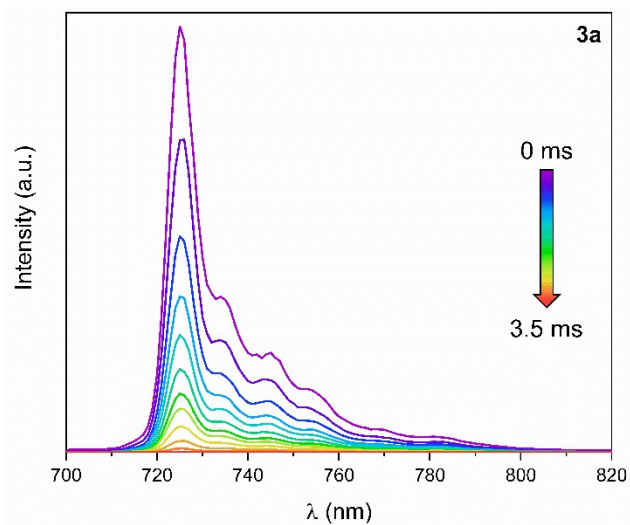


**Figure S10.** Time-delayed phosphorescence spectrum for **3a** in 4:1  $\text{CH}_3\text{CH}_2\text{OH}:\text{CH}_3\text{OH}$  glass at 77 K and varying delay times.

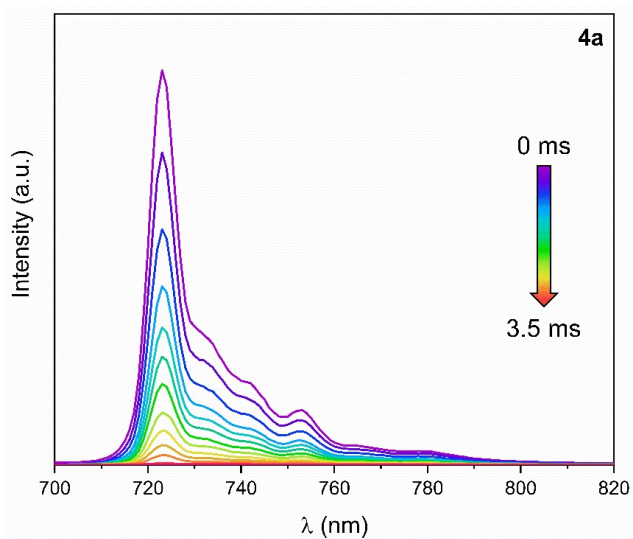


**Figure S11.** Time-delayed phosphorescence spectrum for **4a** in 4:1  $\text{CH}_3\text{CH}_2\text{OH}:\text{CH}_3\text{OH}$  glass at 77 K and varying delay times.

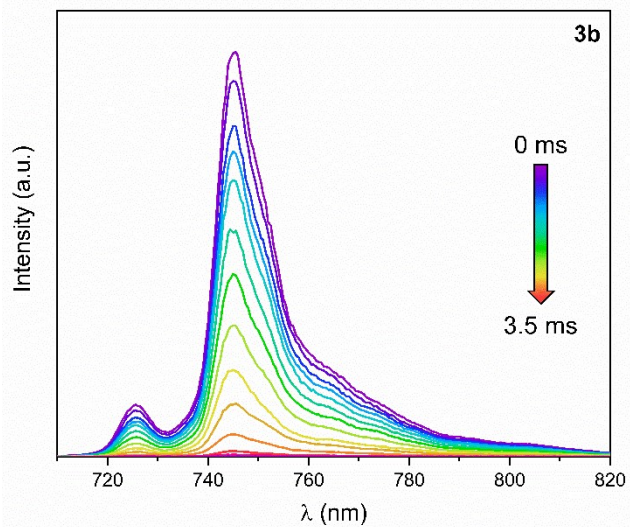


**Figure S12.** Time-delayed phosphorescence spectrum for **3b** in 4:1 CH<sub>3</sub>CH<sub>2</sub>OH:CH<sub>3</sub>OH glass at 77 K and varying delay times.

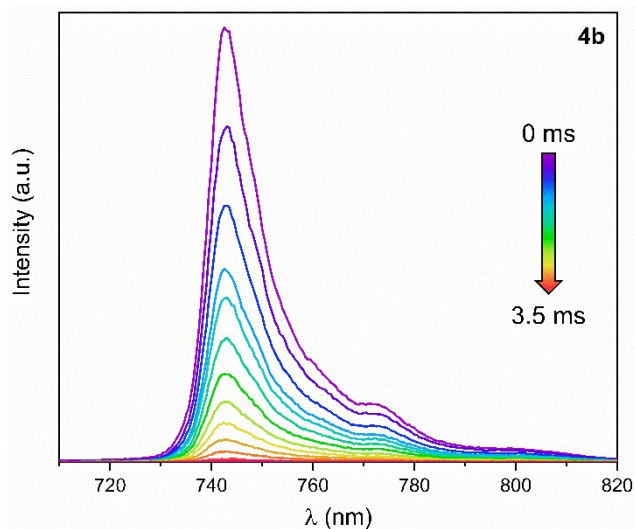


**Figure S13.** Time-delayed phosphorescence spectrum for **4b** in 4:1 CH<sub>3</sub>CH<sub>2</sub>OH:CH<sub>3</sub>OH glass at 77 K and varying delay times.

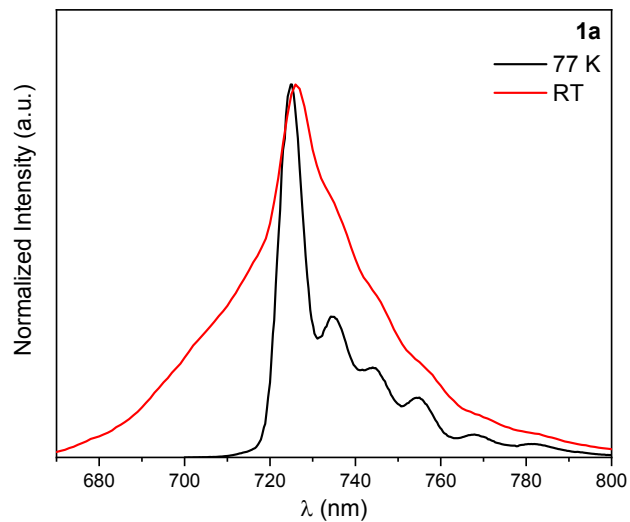


**Figure S14.** Emission spectra of **1a** at RT in degassed  $\text{CH}_3\text{CN}$  and 77 K in 4:1  $\text{CH}_3\text{CH}_2\text{OH}:\text{CH}_3\text{OH}$  glass.

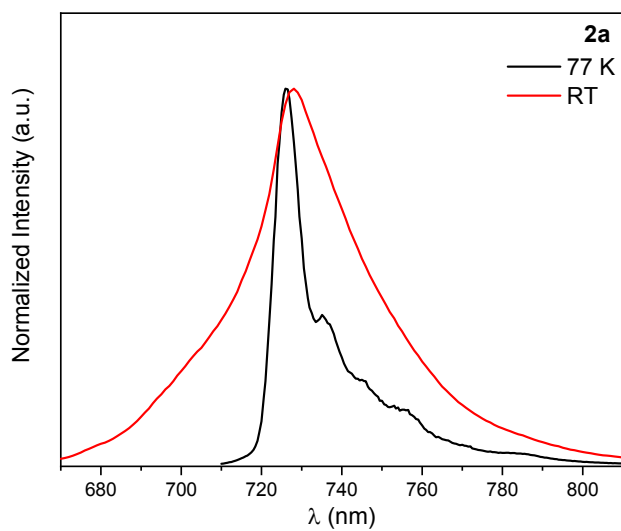


**Figure S15.** Emission spectra of **2a** at RT in degassed  $\text{CH}_3\text{CN}$  and 77 K in 4:1  $\text{CH}_3\text{CH}_2\text{OH}:\text{CH}_3\text{OH}$  glass.



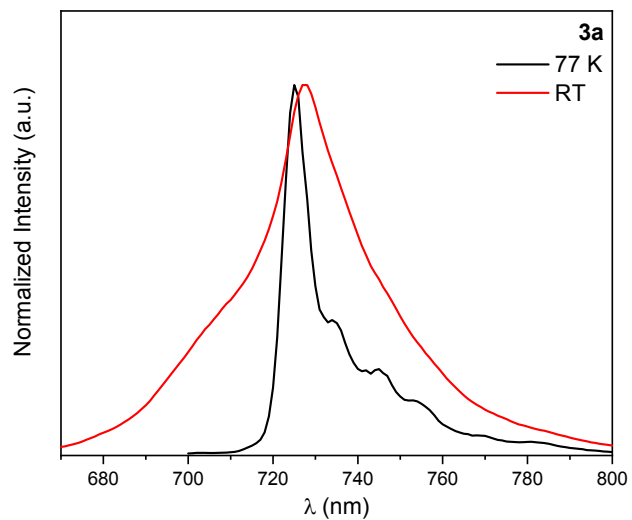


**Figure S16.** Emission spectra of **3a** at RT in degassed  $\text{CH}_3\text{CN}$  and 77 K in 4:1  $\text{CH}_3\text{CH}_2\text{OH}:\text{CH}_3\text{OH}$  glass.

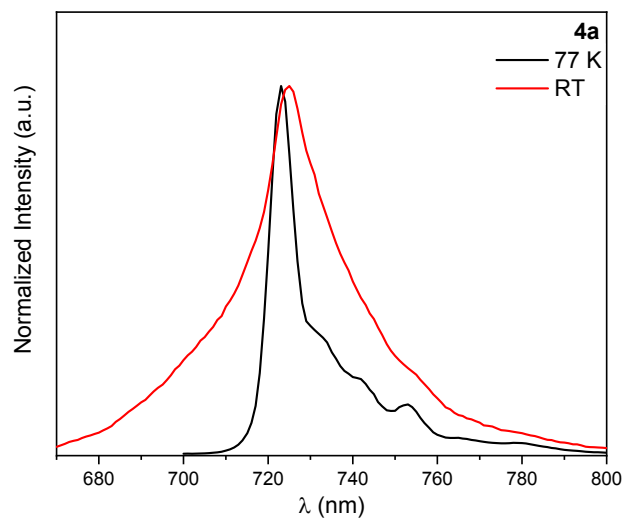


**Figure S17.** Emission spectra of **4a** at RT in degassed  $\text{CH}_3\text{CN}$  and 77 K in 4:1  $\text{CH}_3\text{CH}_2\text{OH}:\text{CH}_3\text{OH}$  glass.

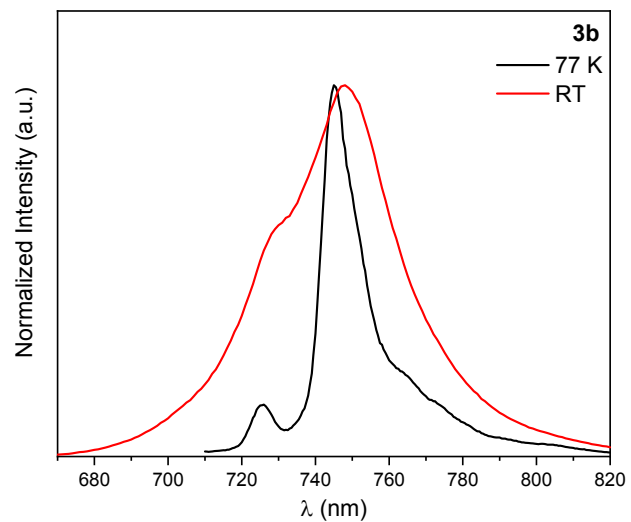


**Figure S18.** Emission spectra of **3b** at RT in degassed  $\text{CH}_3\text{CN}$  and 77 K in 4:1  $\text{CH}_3\text{CH}_2\text{OH}:\text{CH}_3\text{OH}$  glass.

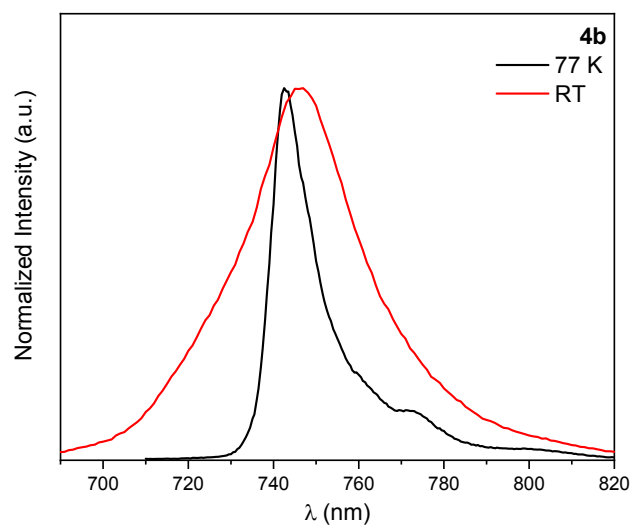


**Figure S19.** Emission spectra of **4b** at RT in degassed  $\text{CH}_3\text{CN}$  and 77 K in 4:1  $\text{CH}_3\text{CH}_2\text{OH}:\text{CH}_3\text{OH}$  glass.

## References

1. Nonius (1998). Collect Users Manual, Nonius Delft, The Netherlands.
2. Z. Otwinowski, W. Minor., *Methods Enzymol.* 1997, **276**, 307–326.
3. P. T. Beurskens, G. Beurskens, R. deGelder, S. Garcia-Granda, R. O. Gould, J. M. M. Smits, *The DIRDIF2008 Program System*, Crystallography Laboratory, University of Nijmegen, The Netherlands: 2008.
4. Bruker (2016). Apex3 v2018.7-2, v2019.1-0, Saint V8.38A, Bruker AXS Inc.: Madison (WI), USA, 2013/2014.
5. a) SHELXTL suite of programs Version 6.14. Bruker Advanced X-ray Solutions. Bruker AXS Inc. 2000-2003, Madison, Wisconsin: USA. b) G.M. Sheldrick, *Acta Cryst. A* 2008, **64**, 112-122.
6. G.M. Sheldrick, *Acta Cryst. A.* 2008, **64**, 112–122.
7. C.B. Hübschle, G. M. Sheldrick, B. Dittrich, *J. Appl. Crystallogr.* 2011, **44**, 1281–1284.
8. G. M. Sheldrick, *University of Göttingen, Germany*, 2016.
9. G. M. Sheldrick, *Crystallogr Sect C Struct Chem.* 2015, **71**, 3-8.